Asociación Argentina de Mecánica Computacional

Mecánica Computacional Vol XXV, pp. 21-40
Alberto Cardona, Norberto Nigro, Victorio Sonzogni, Mario Storti. (Eds.)
Santa Fe, Argentina, Noviembre 2006

COMPUTATIONAL SPINNING MODEL TO STUDY DIFFERENT EXPRESSIONS PROPOSED IN THE LITERATURE FOR THE ELONGATIONAL VISCOSITY EVALUATION FROM SPINNING EXPERIMENTAL DATA

Mariel L. Ottone, Marta B. Peirotti and Julio A. Deiber

Instituto de Desarrollo Tecnológico para la Industria Química
INTEC (UNL - CONICET)
Güemes 3450, S3000GLN - Santa Fe, Argentina, treoflu@ceride.gov.ar

Keywords: Spinning Model, Extensional Viscosity, Rheotens

Abstract. The relation between isothermal elongational flow and other flow kinematics, like shear flow, was of interest since the early stages of rheometry. The main seeking purpose was precisely to achieve the evaluation of the elongational viscosity as a function of elongational rate through other simpler kinematics attained easily in experimental programs and commercial rheometers. At present, it is known that this target is not possible. It is also clear that experimental data of the steady elongational viscosity of viscoelastic melts at different temperatures are quite difficult to obtain. In this sense, various techniques for determining the elongational properties of these materials were developed; the apparatuses involved are considered expensive, difficult to operate and unsuitable for most types of materials, especially for those having a low viscosity. A technique widely used at present dealing with a variety of polymer melts is the isothermal fiber spinning process in its well-known version designated Rheotens. This apparatus presents a challenging problem, which consists in translating measurements of the spinning flow kinematics and filament forces into those variables pertaining to pure elongation flow within the rheometric framework. According to what has been reported in the literature, different research groups have studied this difficult problem and proposed approximate solutions for this purpose. In the present work we use a computational model of isothermal melt spinning to study the different accuracies obtained with expressions suggested in previous works to evaluate the elongational viscosity from spinning experimental data. Some physical aspects concerning the requirements to attain appropriate experimental conditions are provided, mainly those concerning the description of different zones present in the spinning kinematics.

1 INTRODUCTION

The presence of flows with a predominant stretching kinematics is frequent in several polymer processing operations like, for instance, blow molding, film blowing and fiber spinning. Consequently, the appropriate design and control of these operations require the knowledge of characteristic rheometric functions pertaining to the elongational kinematics, like the elongational viscosity as a function of the elongational rate. Various techniques for determining the uniaxial elongational properties of polymer melts have been developed in rheological laboratory (see, for instant, Meissner, 1971), in which samples are stretched under constant stress or constant elongational rate. Nevertheless, one should also observe that these apparatuses are expensive, difficult to operate, and not suitable for all polymers. To obtain an approximate characterization of a polymer melt behavior under a predominant stretching flow, one of the techniques most widely used dealing with a variety of fluids is the isothermal fiber spinning operated, for instance, in the well-known version designated Rheotens (see, for example, Bernnat, 2001; Wagner et al., 1998; Rauschenberger and Laun, 1997; Lin and Hu, 1997; Laun and Schuch, 1989, Bayer 1979). The Rheotens experiment was developed (Meissner, 1971) simultaneously with the uniaxial elongational rheometer. These instruments have in common a system composed of two rotating wheels, which elongate a polymer melt sample with a prescribed velocity producing an elongational deformation. The main differences between them are that the elongational rheometer yields a time dependent uniaxial extension with constant elongational rate, where the polymer sample is initially homogeneous and stress-free (Bernnat, 2001), while the Rheotens is an elongational experiment at a constant prescribed take up velocity / force where the polymer sample tested is initially sheared in a capillary tube. Therefore, in this last apparatus the melt passes through a significant relaxation process, probably in a short distance before entering into a monotonic non-uniform stretching response. This relaxation process involves the well-known swelling zone, where the filament diameter takes a maximum value.

It is relevant to indicate here that measurements carried out in the Rheotens are fast and easy to perform with good reproducibility (Bernnat, 2001). Also the rheological information obtained in this process belongs to the steady state. On the other hand, the elongational rheometer provides the transient elongational viscosity from where the asymptotic steady state values are estimated. Therefore, having into account these practical advantages to characterize polymer melts in the isothermal spinning flow, it was clear that expressions to convert experimental data, obtained as tensile force at the end of the spinline versus take up velocity, into a relation between elongational viscosity and elongation rate was required. In this direction, several proposals are available in the literature (Bayer, 1979; Laun and Schuch, 1989; Revenu et al., 1993; Macosko, 1994; Wagner et al., 1996; Fulchiron et al., 1997; Rauschenberger and Laun, 1997; Lin and Hu, 1997; Wagner et al., 1998). For instance, Laun and Schuch (1989) provided values of the elongational viscosity at the end of the spinline by using the tensile force and the draw ratio, without taking into account swelling effects. These authors found that, in spite of the large number of assumptions considered, the spinning elongational viscosity is in qualitative agreement with the rheometric elongational viscosity at the same temperature and elongational rate, although it is different quantitatively. The observed discrepancy can be attributed in part to the combined effects of inhomogeneous spinning kinematics and cooling along the spinline. Nevertheless, in principle, the spinning elongational viscosity calculated at each point of the filament from an isothermal fiber spinning experiment cannot be considered equivalent to the steady state rheometric elongational viscosity function (Ottone et al., 2006). In fact, the comparison of the spinning and rheometric elongational viscosities needs a careful examination of the experimental conditions. In this sense the influence of the swelling zone should be also analyzed or eliminated appropriately in order to establish the range of elongational rates over which the comparison can be qualitatively achieved (see also, Laun and Schuch, 1989; Revenu et al., 1993; Lin and Hu, 1997).

It is also interesting to point out that Revenu et al. (1993) measured the spinning elongational viscosity of polyethylene through isothermal melt spinning. They measured axially the filament diameter through a photographic technique, and then obtained both the elongational rate and the tensile stress through the mass and force balances in the polymer melt domain. Thus, the spinning elongational viscosity at different points of the extended filament was obtained excluding the effect of the filament swell, and having into account that the elongational rate is not homogeneous. In the work of Lin and Hu (1997), the Rheotens device (Gottfert tensiometer) is utilized to measure the take up force of polymer melts in isothermal spinning flow. They analyzed the approach proposed by Revenu et al. (1993) to evaluate the spinning elongational viscosity, and then proposed another procedure for these calculations by assuming, however, that the filament radius changed linearly along the spinline when the swelling phenomenon was not considered.

It is then clear that the works mentioned above provided procedures and expressions to calculate the spinning elongational viscosity from Rheotens experimental data. In addition, other studies have proposed to include a constitutive equation in these analyses. In this sense, in order to interpret better Rheotens experimental data from the rheometric point of view, various authors have used more complex theoretical models, including numerical calculations, where differential and integral constitutive equations were applied (Sridhar and Gupta, 1991; Petrie and Petrie, 1995; Petrie, 1995; Rauschenberger and Laun, 1997). Petrie and Petrie (1995) and Petrie (1995) proposed that a spinning elongational viscosity could be defined as the ratio of stress to elongational rate at the midpoint of the spinline or as an averaged quantity based on measurable quantities like applied force, flow-rate, spinline length and velocities. More recently Bernnat (2001) tried to use the Wagner integral constitutive equation to interpret these experimental data apart from carrying out a wide and interesting experimental program concerning Rheotens measurements of different polyethylene melts. The numerical method implemented for this purpose resulted quite unstable and the author suggested the need for a different constitutive equation. Based on these conclusions, instead we study below the use of the Phan-Thien and Tanner (PTT) differential constitutive equation for the same purpose of finding a relation between spinning and rheometric elongational viscosities.

At present, it is clear that there is much interest to measure and evaluate the local elongational rate along the spinline by photographing the filament. The target is the estimation of the filament radius gradients for complementary calculations (see for instance, Bayer, 1979; Laun and Schuch, 1989; Revenu et al., 1993). Another possibility is to measure the local velocity along the fiber with the Laser-Doppler Velocimeter. Then from these experimental data the shape of the deformed filament as well as the local elongational rates can be calculated (Wagner et al., 1998; Bernnat, 2001).

In the present work a previous computational non-isothermal spinning model (Ottone and Deiber, 2002) is used, which is adapted here for the isothermal melt spinning flow to compare the spinning and rheometric elongational viscosities through the expressions suggested in previous works. In this specific work the study is carried out with a polyethylene therephtalate (PET), which is a typical polymer used in the commercial production of fibers. The rheological model was taken from Ottone and Deiber (2000), and the rheological parameters pertain to a PET melt reported by Gregory and Watson (1970). Therefore the model proposed previously is evaluated here under isothermal flow conditions to simulate the experimental operation of the Rheotens, and thus to be able to extract the relevant information required to compare the spinning and rheometric elongational viscosities. We thus expect to test the expressions proposed by previous authors with the same purpose.

The present work is organized as follows. First the basic numerical algorithm used to model the spinline is briefly described by using the one-relaxation mode PTT model mentioned above (Section 2). Then, in Section 3, aspects on the numerical solution of the spinning model are presented. We also define both the spinning elongational viscosity and the rheometric elongational viscosity, and express the clear differences between them in Section 4. In the Results and Discussion section, different expressions proposed previously to compare these viscosity functions are analyzed and discussed by using numerical data provided by the numerical algorithm that simulates the isothermal spinning test. Finally some relevant conclusions and proposal for further researches are provided.

2 BASIC EQUATIONS FOR THE SPINNING FLOW

The spinning flow is formulated in the steady state regime (Figure 1). The basic tensorial model to obtain the resulting equations of the perturbed model presented by Ottone and Deiber (2002) is briefly described here.

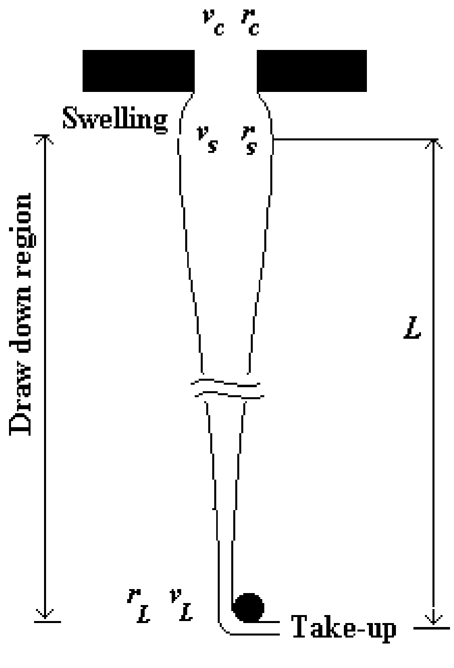

Figure 1: Scheme of isothermal melt spinning.

Since the polymer is considered incompressible, the mass balance implies,

$$\left(\underline{\nabla} \cdot \underline{v}\right) = 0 \tag{1}$$

where $\underline{v}$ is the velocity vector. The balance of momentum in the filament is expressed,

$$\rho \underline{v} \cdot \underline{\nabla} \underline{v} = -\underline{\nabla} p + \underline{\nabla} \cdot \underline{\underline{\tau}} + \rho \underline{g} \tag{2}$$

where ρ is the polymer density, p is the pressure field, $\underline{g}$ is the gravity vector and $\underline{\underline{\tau}}$ is the extra stress tensor considered symmetric throughout this work. Since the spinning flow is required for isothermal conditions, the energy balance in the filament is not included in this study. Thus it is assumed that the mechanical power $\underline{\underline{D}} : \underline{\underline{\tau}}$ is relatively small and the temperature field is approximately constant. Here $\underline{\underline{D}} = \left(\underline{\nabla} \underline{v} + \underline{\nabla} \underline{v}^T\right)/2$ is the rate of deformation tensor, which is a function of the fluid kinematics. Throughout this work v is used to designate the axial velocity component of the velocity vector in the cylindrical coordinate system.

The appropriate set of boundary conditions to solve Eqs. (1) to (2) are taken directly from Denn (1983). In addition, since the PTT model is considered with the retarded elastic response, the asymptotic Newtonian term $\underline{\underline{\tau}}_s = 2\eta_s \underline{\underline{D}}$ is included (see also below). We fix the origin of the coordinate system at the maximum swelling of the polymer melt, where the jet forms at the exit of the extrusion capillary. Therefore throughout this work we designate initial conditions to the boundary conditions at *z*=0, which are,

$$\begin{aligned} &v = v_s, \qquad T = T_o, \qquad \tau_s^{zz} = \tau_s^{rr} = 0 \\ &r_o(0) = r_s, \qquad \tau^{zz} = \tau_o^{zz}, \qquad Rel = \frac{\tau^{rr}}{\tau^{zz}} \end{aligned} \tag{3}$$

where $r_o(z)$ is the fiber radius as a function of the axial direction *z*, v_s is the melt velocity at the maximun swelling with radius r_s and T_o is the extrusion melt temperature which is kept constant along the filament. Therefore $v_s = v_c r_c^2 / r_s^2$, where v_c is the melt averaged velocity in the extrusion capillary of radius r_c (the value of r_s is around $r_c\sqrt{2}$ according to George, 1982). Also the stress ratio *Rel* can be varied in the range $-0.5 < Rel < 0$ for viscoelastic fluids. This result has been fully discussed in the literature (Denn, 1983), where it was reported that numerical solutions were not sensitive for values of *Rel* within this specific range, and that the condition $Rel \approx 0$ is a good approximation (Ottone and Deiber, 2000).

The take up boundary conditions at $z = L$ are,

$$v = v_L, \qquad T = T_o \tag{4}$$

Once the stress field is known at this position of the filament, one obtains $F_L^{eff} = (\tau^{zz} - \tau^{rr})_L (\pi r_c^2)/DR$, where $DR = v_L / v_c$ is the spinning draw ratio. Also, F_L^{eff} is the effective tensile force at the take up position in the spinline. This force is calculated as the resultant of all forces existing in the filament at position $z = L$. Thus most of the theories to be tested below evaluate $F_L^{eff} = F_L + F_{ST} + F_I + F_G$, where F_L is the take up force measured experimentally and ($F_{ST} + F_I + F_G$) is calculated by considering other forces coming from surface tension, inertia and gravity, respectively (see, for instance, Macosko, 1994). It is appropriate to point out here that different draw ratios may be defined in the spinning process apart from *DR*. In fact, $DR' = v_L / v_s$ involves the swelling velocity and $DR_s = v_s / v_c$, consequently $DR = DR' DR_s$.

In addition, the stress tensor $\underline{\underline{T}} = -p\underline{\underline{\delta}} + \underline{\underline{\tau}}$ involves the extra stress tensor $\underline{\underline{\tau}}$ and the pressure *p*, where $\underline{\underline{\delta}}$ is the unit tensor. To complete the formulation of the spinning model, the viscoelastic stress $\underline{\underline{\tau}}_p$ is required, which is a part of the total extra stress tensor $\underline{\underline{\tau}} = \underline{\underline{\tau}}_p + \underline{\underline{\tau}}_s$, where $\underline{\underline{\tau}}_s = 2\eta_s \underline{\underline{D}}$ is associated to retardation effects. In this sense, one expresses,

$$\underline{\underline{\tau}}_p + \lambda \frac{\delta}{\delta t} \underline{\underline{\tau}}_p = 2\lambda G \underline{\underline{D}} \tag{5}$$

for the Phan-Thien and Tanner model (PTTM). In Eq. (5), the expression,

$$\frac{\delta}{\delta t} \underline{\underline{\tau}}_p = \frac{D}{Dt} \underline{\underline{\tau}}_p - \underline{\underline{L}} \cdot \underline{\underline{\tau}}_p - \underline{\underline{\tau}}_p \cdot \underline{\underline{L}}^T - \underline{\underline{\tau}}_p \frac{D\ln T}{Dt} \tag{6}$$

is the Gordon-Schowalter (1972) non-affine time-convective derivative, where the effect of the thermal history is accounted through the term $D\ln T / Dt$, although for the case of isothermal spinning is null. Also $\underline{\underline{L}} = \underline{\nabla} \cdot \underline{v} - \chi \underline{\underline{D}}$ is the effective velocity gradient tensor. We define $\eta_s = \eta_p (1-\alpha)/\alpha$ and $\eta_p = \lambda G$, and the instantaneous elastic response can be obtained for $\alpha = 1$ (Denn, 1990).

For the PET under study, Gregory and Watson (1970) reported the following expression of the relaxation time: $\lambda_o = 0.016\, exp[-11.9755 + 6802/(T + 273)]$. In particular, the PTT model considers a relaxation time that is a function of the stress tensor expressed $\lambda = \lambda_o(T)/K(T, tr\underline{\underline{\tau}})$ where $K = exp[\xi\, tr\underline{\underline{\tau}} / G]$. In this context of analysis the relaxation modulus changes with temperature according to $G = G_o\,(T/T_r)$ where T_r is the reference temperature. These expressions are useful to compute the rheological model at the same temperature as that of the spinning flow. The rheometric characterization of the PTT rheological model is also taken from Ottone and Deiber (2000). Thus rheological parameters of the PET melt (case study of this work) are: $G_o \approx 5246$ Pa, $\alpha \approx 0.8$, $\chi \approx 4\ 10^{-5}$ and $\xi \approx 9.25\ 10^{-5}$.

3 ASPECTS ON THE NUMERICAL SOLUTION OF THE SPINNING MODEL

In this section, the main numerical steps followed to solve the spinning model described above are presented only. A detailed description of the algorithm used here may be found in Ottone and Deiber (2000 and 2002). Thus, a regular perturbation analysis is applied to Eqs. (1) to (6) according to the scheme proposed by Henson et al. (1998). In this step one obtains the 2-D perturbed model. This scheme allows one to neglect rigorously terms of small orders from the balance and constitutive equations and the boundary conditions of the complete model (see Section 2). Then the perturbed 2-D model is averaged in the radial direction of the filament, without any approximation, to yield an appropriate version of the perturbed average model. One should also observe that the complete model described by Eqs. (1) to (6) may be expressed in dimensionless form by using appropriate scales (Henson et al. (1998)). Thus, the perturbation analysis is carried out on the dimensionless model. Therefore any dependent variable, represented by P in the generalized sense, can be expressed $P = \sum_{n=0}^{\infty} \Lambda^n P^{(n)} = P^{(o)} + \vartheta(\Lambda)$, where Λ is the ratio between the capillary radius and the stretching length of the filament. In the regular perturbation analysis, terms of order Λ and greater are neglected to introduce the slenderness hypothesis. The perturbed averaged model thus obtained can be expressed in the matrix form $\dot{\underline{x}} = \underline{\underline{A}}^{-1}(\underline{x}) \cdot \underline{b}$ where $\dot{\underline{x}} = \left\{ \frac{\partial v}{\partial z}, \frac{\partial f}{\partial z}, \frac{\partial \underline{\underline{\tau}}}{\partial z} \right\}$ and $f = \frac{dv}{dz}$. Equation $\dot{\underline{x}} = \underline{\underline{A}}^{-1}(\underline{x}) \cdot \underline{b}$ can be solved with the appropriate initial conditions for velocity, temperature and stresses as reported above. Nevertheless, in practice one may know the value of the axial velocity v_s at the initial position as well as the melt temperature at the extrusion capillary only. Unfortunately, the initial stresses are not known beforehand and they must be found through a numerical iterative process already described in the literature (see, for instance, Papanastasiou et al., 1996). In the framework of cylindrical coordinates r and z, the iterative process consists of initializing the viscoelastic tension components τ_p^{zz} and τ_p^{rr} at $z = 0$ (this position is placed at the maximum swelling of the filament) and solving the system of equations described above iteratively with the fourth order Runge-Kutta method, until one reproduces the value assigned to v_L at $z = L$, with the following convergence criterion $\left| v^k - v_L \right| / \left| v_L \right| \leq 10^{-6}$,where k indicates the number of axial step size used to reach L. Thus a two-point-boundary value problem is solved.

In addition, it is know that only one stress, say $\tau_p^{zz}(0)$, at the initial condition shall be iterated while the other is fixed with a constant ratio $Rel = \tau_p^{rr} / \tau_p^{zz}$ at $z = 0$. Since in our model we consider, in addition to previous works, the constitutive equation of Phan-Thien and Tanner with retarded response, the initial value $f = 0$ is also required, which is the best estimate for the velocity derivative at the maximum extrudate swell (Ottone and Deiber, 2000).

The numerical code is written in FORTRAN language, and the axial step size is fixed at 10^{-5} m. This value is small enough to achieve appropriately the convergence criterion concerning the take up velocity v_L with a running time of around 20 minutes, when a PC Pentium III is used. Numerical results of rheometric and spinning viscosities are precise enough to test the theories under consideration below.

4 RHEOMETRIC AND SPINNING ELONGATIONAL VISCOSITIES

The purpose of this section is to define the rheometric η_e and spinning ${\eta_e}^p$ elongational viscosities, which are used in the Results and Discussion section below. As described above, while the first viscosity is a rheometric function under isothermal conditions, the second one is obtained from the isothermal melt spinning process. Therefore, throughout this work, the use of a super-index p indicates that variables are evaluated with the melt spinning model to distinguish their values from those under strict rheometric conditions. It is also clear that the spinning process variables $\eta_e{}^p$ and $\dot{\varepsilon}^p$ cannot be superposed in the rheometric elongational map defined by the elongational viscosity η_e versus the elongational rate $\dot{\varepsilon}$ for different parametric temperatures T without further considerations.

Since a cylindrical coordinate system is used with the z-axis along the filament from the maximum swelling to the take up roll (Figure 1), the spinning elongational viscosity, which varies along the spinline, is expressed at $z = L$ as follows:

$$\eta_e^p = \frac{(\tau^{zz} - \tau^{rr})_L}{\dot{\varepsilon}^p} = \frac{F_L^{eff}\, DR}{\pi\, r_c^2 \dot{\varepsilon}^p} \tag{7}$$

where the true spinning elongational rate is $\dot{\varepsilon}^p = \left(\dfrac{\partial v}{\partial z}\right)^p$, and it varies with coordinate z. Nevertheless, the theories to be analyzed below provide an estimate $\dot{\varepsilon}^p$ through a proposed relationship involving the process variables. In this work in particular we evaluate numerically F_L^{eff} from the model proposed above for a given set of process variables and apply directly the theories proposed for appropriate comparisons. In particular, in the equations proposed by Bayer (1979), Revenu et al. (1993) and Wagner et al. (1998), the knowledge of the experimental fiber radius $r_o(z)$ and axial velocity profile $v(z)$, respectively, are required along the spinline. For these cases we provide these profiles through numerical calculations in order to be able to carry out the expected comparisons among theories. After using the above relationships, it is then clear that the spinning elongational viscosity evaluated at $z = L$ may be also expressed as follows:

$$\eta_e{}^p(\dot{\varepsilon}^p) = \frac{F_L^{eff}}{\dot{\varepsilon}^p \pi\, r_L^2} \tag{8}$$

where r_L is the value of $r_o(z)$ at $z = L$. Thus, the central problem here is to evaluate $\dot{\varepsilon}^p$ to be able to compare the values of η_e^p and η_e. We show in this work that these functions may be either rather close or quite different depending on the range of values selected for the process variables as well as the semi-empirical expression used to calculate $\dot{\varepsilon}^p$.

Before ending this section, it is also appropriate to define here the rheometric elongational viscosity,

$$\eta_e(\dot{\varepsilon}) = \frac{\left(\tau^{zz} - \tau^{rr}\right)}{\dot{\varepsilon}} \tag{9}$$

where $\dot{\varepsilon} = \dfrac{\partial v}{\partial z}$ must be constant throughout the elongational rheometer. As pointed out above, it was clear that η_e^p should not be equal to η_e due to the effect of non-uniforms values taken by $\dot{\varepsilon}^p$ along the spinline.

5 RESULTS AND DISCUSSION

In this section we analyze different equations proposed previously in the literature to calculate $\dot{\varepsilon}^p$, once F_L^{eff} and $r_o(z)$ have been obtained from spinning experimental data. In this work F_L^{eff} and $r_o(z)$ are, however, obtained numerically within the framework of a tensorial constitutive equation solved for the rheometric and spinning processing conditions. Thus by using Section 2, we consistently simulates the spinning experimental data in order to apply the results in the previous proposed expressions to be tested in this work. It is clear that by introducing a tensorial constitutive equation as representing a given material, one can obtain rigorously the response under different flow conditions of this material, and hence be able to evaluate the quality of approximate expressions that intent to relate functions associated to different flow kinematics, like for instance the relationship between η_e^p and η_e. This procedure is an effective test and validation of those expressions proposed in the literature to relate these material functions.

5.1 Expressions proposed by Bayer (1979)

The model of Bayer (1979) has also been used by Laun and Schuch (1989), and Rauschenberger and Laun (1997). This author expressed the elongational rate at $z = L$ as a function of the draw ratio $DR = \dfrac{v_L}{v_c} = (\dfrac{r_c}{r_L})^2$. Thus with the help of a photographic technique the filament radius was obtained along coordinate z to deduce the following equation,

$$\dot{\varepsilon}^p = \frac{v_c}{L} DR \ln\left(S_2 \; DR\right) \tag{10}$$

where the local transversal area of the filament is assumed to vary exponentially with z.

In Eq. (10), S_2 is a free parameter related to the filament swelling. Figure 2 shows the comparison of η_e^p and η_e as obtained from Eqs. (7), (9) and (10), when v_L is varied from 300 to 3500 m/min. This figure also shows the effect of different values of S_2 for a fixed value of the extrusion velocity (v_c= 0.606 m/s) and L = 19 cm. In general, one finds that for very low values of S_2, η_e^p approximates η_e for the range of low elongational rates used. The converse is also true; thus for high S_2 this approximation is satisfied at relatively high values of elongational rates. Further, our numerical tests indicate that there is not an optimum value fitting well all the experimental data provided in the take up velocity range used here. In addition, for $S_2 \approx 0.1$ it was not possible to evaluate η_e^p with Bayer equations for $v_L < 800$ m/min (DR=22) indicating that this parameter provides realistic $\dot{\varepsilon}^p$ only in a limited range of take up velocities.

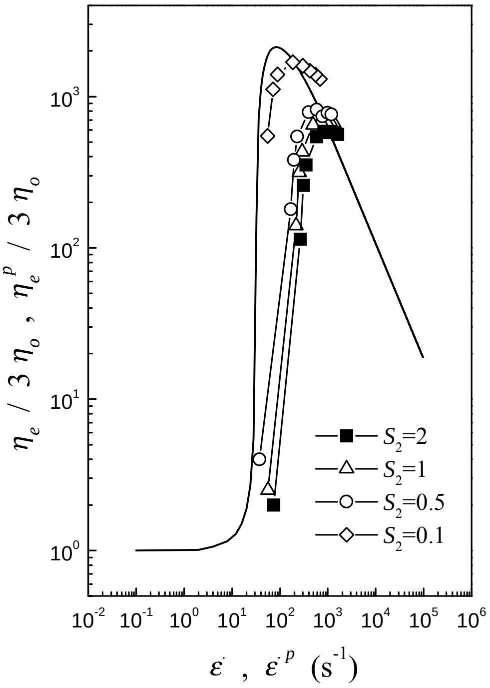

Figure 2: Rheometric and spinning elongational viscosities as functions of rheometric and spinning elongational rates. Symbols are the predictions of the spinning elongational viscosity through the expressions proposed by Bayer (1979) for different values of S_2. Also v_c= 0.606 m/s and $L =$ 19 cm. The rheometric elongational viscosity (full line) is predicted with the tensorial constitutive equation. The take up velocities are in the range v_L = 300 to 3500 m/min.

5.2 Expressions proposed by Revenu et al. (1993)

This model presented by Revenu et al. (1993) also requires the evaluation of the filament radius along the spinline through a photographic technique. These authors proposed to use the sum of two exponential functions to represent $r_o^2(z)$ when the swelling zone is excluded. Nevertheless, for the PET melt studied here, we found that for high draw ratios this proposal is not necessarily the appropriate one, and hence another function is required. Therefore we tested this model for 300 $\leq v_L \leq$ 3500 m/min ($8 \leq DR \leq 96$) and found that only for DR=8 the filament radius may be fitted to the following expression as suggested by Revenu et al. (1993) for different polymers,

$$r_o^2(z) = A\exp(-B\,z) + C\exp(-D\,z) \tag{11}$$

where A=-0.04708 m^2, $B=0$, C= 3.00392 m^2 and D=12.45180 m^{-1}. Consequently the spinning elongational rate at $z = L$ is,

$$\dot{\varepsilon}^{p} = \frac{Q}{\pi} \frac{A\,B \exp\left(-B\,L\right) + CD \exp\left(-D\,L\right)}{\left[A \exp\left(-B\,L\right) + C \exp\left(-D\,L\right)\right]^{2}} \tag{12}$$

Also, for 22 $\leq DR \leq$ 96 the following expression was required,

$$r_o^{\,2}(z) = \frac{1}{(A + B\,\exp(z))} \tag{13}$$

where A and B are reported in Table 1.

DR	A (m^{-2})	B (m^{-2})	Regression Coefficient
22.0	-62.33	62.64	0.9999
24.7	-64.07	64.38	0.9999
27.5	-65.19	65.51	0.9999
41.3	-67.18	67.49	0.9995
55.0	-67.76	68.06	0.9993
68.8	-68.02	68.33	0.9992
82.5	-68.04	68.35	0.9991
96.0	-68.11	68.42	0.9991

Table 1: Fitting parameters for Eq. (13) at different values of draw ratio ($22 \leq DR \leq 96$)

Therefore the elongational rate at the filament take up for this range of *DR* is,

$$\dot{\varepsilon}^{p} = \frac{Q}{\pi} B \exp(L) \tag{14}$$

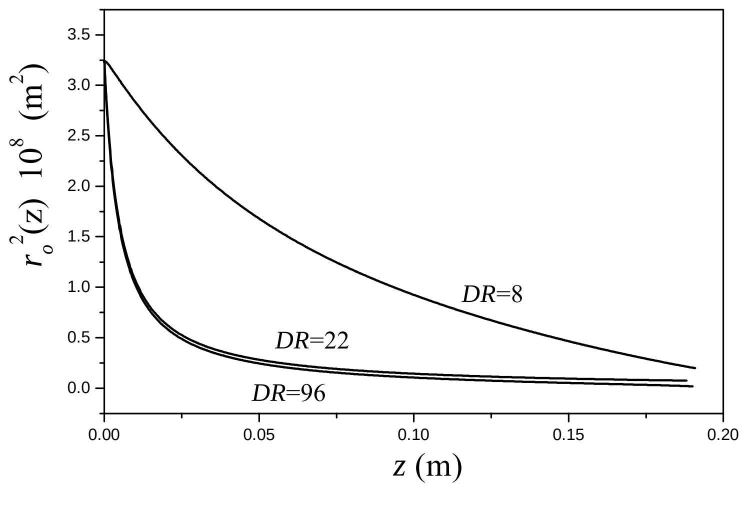

Figure 3: Numerical predictions of $r_o^2(z)$ with the isothermal spinning model for different draw ratios. Take up velocities are in the range v_L = 300 to 3500 m/min. Also v_c = 0.606 m/s and L = 19 cm.

Figure 3 shows numerical values of $r_o^2(z)$ for $DR =$ 8, 22 and 96 obtained from the spinning model described by Eqs. (1) to (6). Thus, from this figure one infers that very low precision may be obtained by measuring experimentally the filament radius at relatively high values of DR, indicating thus that in practice this model provides acceptable results at low values of draw ratio only (*DR*<22). This conclusion is evident in Figure 4, where the rheometric and spinning elongational viscosities are presented as functions of the rheometric and spinning elongational rates for different take up velocities. It is observed that at high values of *DR*, Eqs. (7), (9), (12) and (14) predict values of η_e^p quite different from η_e for the PET melt under study. This may be a consequence of the difficulties found to fit the values of fiber filament radius for *DR*>22, where experimental values describing profiles $r_o^2(z)$ are too close one another.

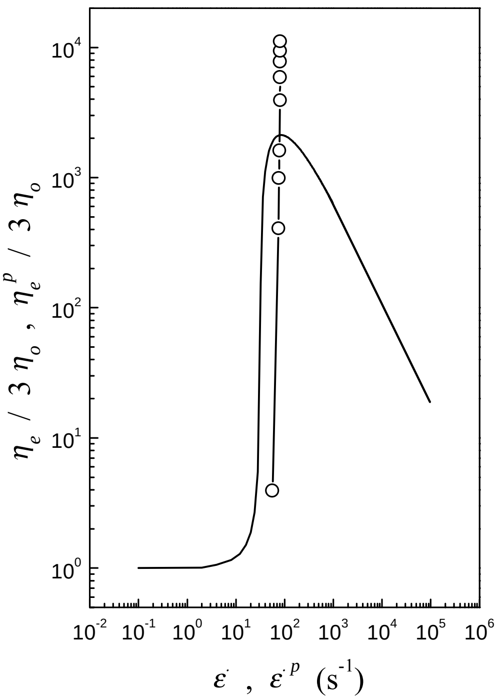

Figure 4: Rheometric and spinning elongational viscosities as functions of rheometric and spinning elongational rates. Symbols are the predictions of the spinning elongational viscosity through the expressions proposed by Revenu et al. (1993). Also v_c = 0.606 m/s and $L =$ 19 cm. The rheometric elongational viscosity (full line) is predicted with the tensorial constitutive equation. The take up velocities are in the range v_L = 300 to 3500 m/min.

5.3 Expressions proposed by Macosko (1994)

The model proposed by Macosko (1994) introduces an average value of the elongational rate $\dot{\varepsilon}^p$ along the filament, which is defined,

$$\dot{\varepsilon}^p = \frac{v_L - v_c}{L} \tag{15}$$

Figure 5 shows the rheometric and spinning elongational viscosities as functions of the rheometric and spinning elongational rates for different take up velocities when Eqs. (7), (9) and (15) are used. It is observed that at relatively low values of *DR*, these equations predict values of η_e^p quite close to η_e for the PET melt under study. Thus in this range of *DR* the use of an average elongational rate (Eq. (15)) seems appropriate to estimate the rheometric elongational viscosity when experimental data of F_L^{eff} are available. Nevertheless, the differences between these viscosities become higher as the *DR* is substantially increased. The predictions of this model are quite similar to those found with Bayer model for low S_2.

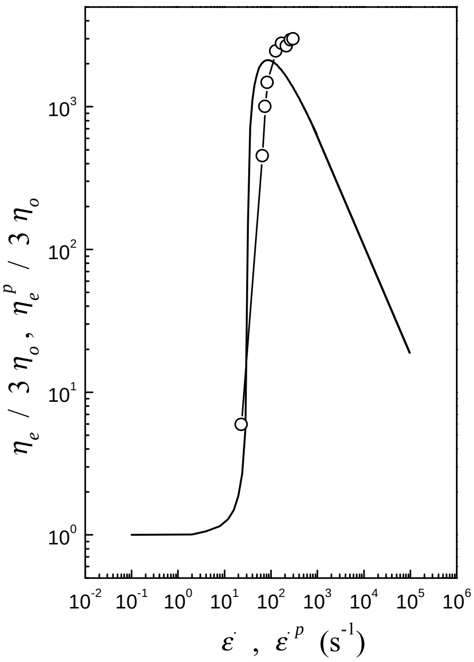

Figure 5: Rheometric and spinning elongational viscosities as functions of rheometric and spinning elongational rates. Symbols are the predictions of the spinning elongational viscosity through the expressions proposed by Macosko (1994). Also v_c = 0.606 m/s and $L =$ 19 cm. The rheometric elongational viscosity (full line) is predicted with the tensorial constitutive equation. The take up velocities are in the range v_L = 300 to 3500 m/min.

5.4 Expressions proposed by Lin and Hu (1997)

The model proposed by Lin and Hu (1997) neglects the swelling zone and considers that the filament radius decreases linearly with *z*. The take up force is obtained with a Rheotens instrument for different polymer melts. These authors proposed a simple expression for the elongational rate by using a similar theoretical analysis as that already presented by Revenu et al. (1993), which is,

$$\dot\varepsilon^p = \frac{2v_c}{L} DR\left(\sqrt{DR}-1\right) \tag{16}$$

Figure 6 shows the rheometric and spinning elongational viscosities as functions of the rheometric and spinning elongational rates for different take up velocities when Eqs. (7), (9) and (16) are used. It is observed that only at relatively high values of *DR*, these equations predict values of η_e^p quite close to η_e for the PET melt under study.

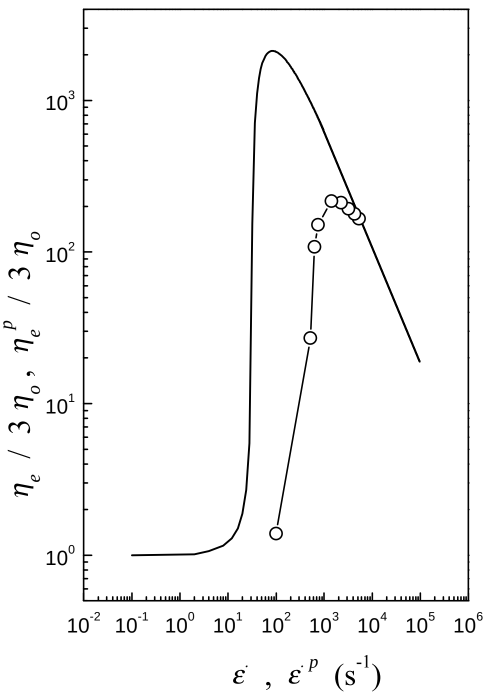

Figure 6: Rheometric and spinning elongational viscosities as functions of rheometric and spinning elongational rates. Symbols are the predictions of the spinning elongational viscosity through the expressions proposed by Lin and Hu (1997). Also v_c= 0.606 m/s and $L =$ 19 cm. The rheometric elongational viscosity (full line) is predicted with the tensorial constitutive equation. The take up velocities are in the range v_L = 300 to 3500 m/min.

5.5 Expressions proposed by Wagner et al. (1998)

The model presented by Wagner et al. (1998) is based on the following experimental evidence, which indicates that when the filament velocity along the spinline is measured by optical methods, it is observed that the velocity increases linearly with *z* below a critical draw ratio, while for higher draw ratios the velocity increases over-proportionally (power-law dependence) with *z*. Therefore, the following expressions are proposed for the two flow regimes:

Linear Regime:

This regime applies for $DR \leq DR_c$, where $DR_c = v_L^c / v_c$ is designated the critical draw ratio, and it corresponds to the limit value of draw ratio above which the filament velocity is not anymore near linear with z. Consequently, in this regime it is evident that v is assumed to increase linearly with *z*. Thus at *z*=*L*,

$$\dot{\varepsilon}^p = \frac{(v_L - v_s)}{L} \tag{17}$$

It is also assumed that the take up force increases linearly with *z* below DR_c. Therefore the spinning elongational viscosity is expressed,

$$\eta_e^p = \frac{\sigma_c}{(v_c / L)(DR_c - DR_s)}\left(\frac{DR}{DR_c}\right) \tag{18}$$

where $\sigma_c = (\tau^{zz} - \tau^{rr})_c = F_L^{eff}(DR_c)/(\pi r_c^2)$ is the stress difference at $z = L$ evaluated for DR_c (we obtain σ_c, of course, from the spinning model formulated through Eqs. (1) to (6)). In Eq. (18), $DR_s = v_s / v_c$ is the draw ratio between swelling and capillary velocities (in practice is a fitting parameter).

Nonlinear Regime:

This regime applies for $DR > DR_c$, and v increases over-proportionally with *z*. Therefore the authors deduced the following expressions at $z = L$ by using the Power Law model with a power index *n*<1,

$$\dot{\varepsilon}^p = v_c \frac{(DR_c - DR_s)}{L}\left(\frac{DR}{DR_c}\right)^{\frac{1}{n}} P(DR) \tag{19}$$

where,

$$P(DR) = 1 + \frac{n}{(n-1)}\frac{DR_c}{(DR_c - DR_s)}\left[\left(\frac{DR}{DR_c}\right)^{\frac{n-1}{n}} - 1\right] \tag{20}$$

Also the spinning elongational viscosity is expressed,

$$\eta_e^p = \frac{\sigma_c}{(v_c / L)(DR_c - DR_s)}\left(\frac{DR}{DR_c}\right)^{\frac{n-1}{n}} \tag{21}$$

Thus this model has three fitting parameters: *n*, DR_s and DR_c (σ_c is an experimental data for the processing conditions at DR_c calculated in this work through the spinning numerical model described through Eqs. (1) to (6)). The critical velocity v_L^c defining DR_c is required to obtain the spinning elongational viscosity as a function of the spinning elongational rate through Eqs. (17) to (21). In this sense, Figure 7 presents velocity profiles for 800 $\leq v_L \leq$ 3500 m/min ($22 \leq DR \leq 96$). It is observed that by following the analysis of Wagner et al. (1998) the critical velocity is around 1000 m/min. Figure 8 reports alternatives concerning the values of v_L^c.

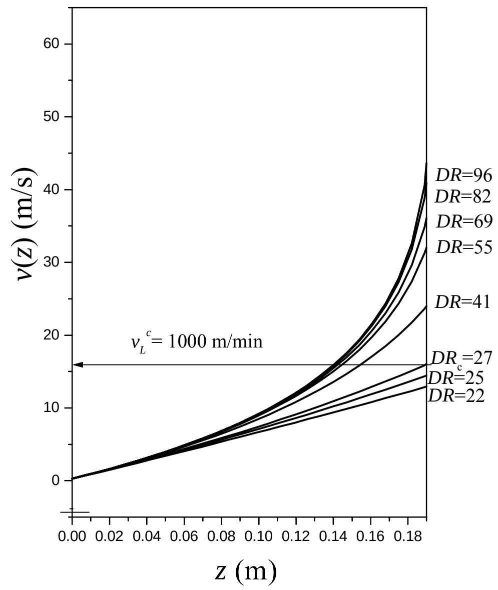

Figure 7: Axial velocity $v(z)$. The take up velocities are in the range v_L = 800 to 3500 m/min. Also v_c = 0.606 m/s and L = 19 cm.

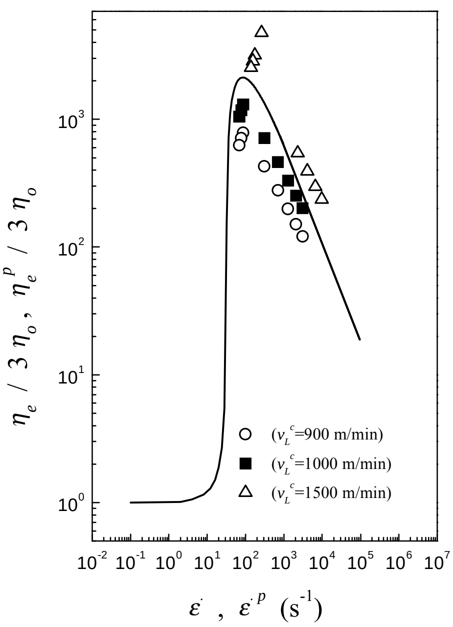

Figure 8: Rheometric and spinning elongational viscosities as functions of rheometric and spinning elongational rates. Symbols are the predictions of the spinning elongational viscosity through the expressions proposed by Wagner et al. (1998). Also v_c = 0.606 m/s and $L =$ 19 cm. The rheometric elongational viscosity (full line) is predicted with the tensorial constitutive equation. The take up velocities are in the range v_L = 800 to 3500 m/min. The effect of v_L^c is illustrated for n =0.4 and DR_S =0.5.

Figure 7 shows the effect of selecting different v_L^c around the value 1000 m/min on the spinning elongational viscosity when n =0.4 and DR_s=0.5, which are kept constant. At each value of the critical velocity a set of values for DR_c and σ_c at $z = L$ are required. Figure 8 shows that as v_L^c takes values different from 1000 m/min, the spinning elongational viscosity differs from the rheometric elongational viscosity.

Figure 9 shows the effect of n on the spinning elongational viscosity when v_L^c=1000 m/min and DR_s=0.5. One observes here that when n increases, different trends of the spinning elongational viscosity predicted by the Nonlinear Regime are obtained, although it is difficult to ascertain which is the appropriate value for this parameter. In principle, it seems that $n = 0.62$ is better and it coincides with that value reported by Wagner et al. (1998) for different polyethylene melts.

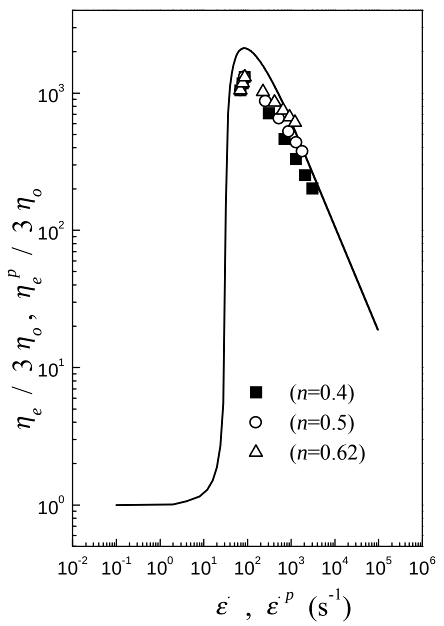

Figure 9: Rheometric and spinning elongational viscosities as functions of rheometric and spinning elongational rates. Symbols are the predictions of the spinning elongational viscosity through the expressions proposed by Wagner et al. (1998). Also v_c= 0.606 m/s and $L =$ 19 cm. The rheometric elongational viscosity (full line) is predicted with the tensorial constitutive equation. The take up velocities are in the range v_L = 800 to 3500 m/min. The effect of n is illustrated for DR_s=0.5 and v_L^c = 1000 m/min.

Figure 10 presents the spinning elongational viscosity for different values of DR_s, when n and v_L^c are constant. It is relevant to observe here that the effect of DR_s on these calculations is not important, at least for $0.5 < DR_s < 1$. From different parametric studies carried out with this model, we found that for the PET melt under study, n= 0.62, DR_s=0.5 and v_L^c=1000 m/min (DR_c=27) are appropriate values to model a spinning elongational viscosity that approximate the rheometric elongational viscosity for the operating conditions indicated in figures.

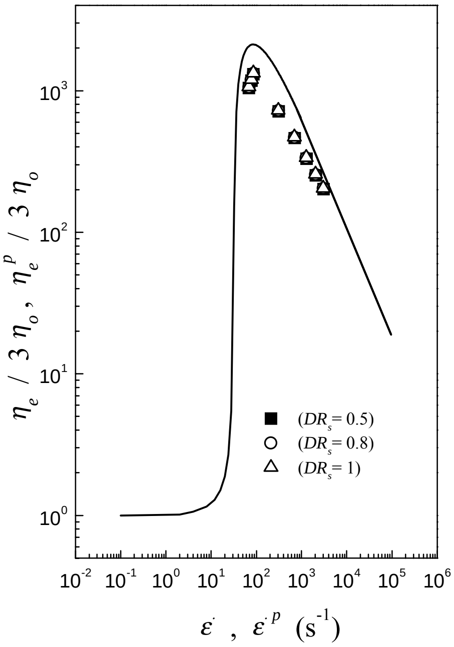

Figure 10: Rheometric and spinning elongational viscosities as functions of rheometric and spinning elongational rates. Symbols are the predictions of the spinning elongational viscosity through the expressions proposed by Wagner et al. (1998). Also v_c= 0.606 m/s and $L =$ 19 cm. The rheometric elongational viscosity (full line) is predicted with the tensorial constitutive equation. The take up velocities are in the range v_L = 800 to 3500 m/min. The effect of DR_s is illustrated for n =0.4 and v_L^c = 1000 m/min.

6 CONCLUSIONS

The isothermal melt spinning model is a useful computational tool to test and validate different expressions suggested in the literature in order to compare the rheometric and spinning elongational viscosities. It is basically concluded that most of the expressions of the spinning elongational rate reported by several authors are good estimates to evaluate the spinning elongational viscosity that qualitatively presents the same trend as the rheometric elongational viscosity. It is also clear that these estimates are not necessarily the local values of the true elongational rates along the spinline, the values of which are also available from numerical calculations with the isothermal spinning model. In addition, one should not expect a quantitative agreement between the elongational viscosities under analysis due to the non-uniform elongational rate field in the spinline. From the expressions analyzed above, one expects to find practical mainly those that do not contain free parameters, even in the cases that less precision may be obtained. In general, the Rheotens data, for instance, may be a powerful tool to characterize qualitatively the extensional response of non-Newtonian fluid.

At present, further researches are required to interpret better how to exclude the complex swelling zone in theoretical analyses. Also, since both the velocity along the spinline and the effective take up force might be measured quite well within the present state of the art of the isothermal spinning process, future researches should focus on the relationship between the spinning elongational viscosity and the true spinning elongational rate, perhaps abandoning the estimation of a representative average spinning elongational rate used in different expressions along the present work. In this sense, we believe that computational models of isothermal fiber spinning may contribute substantially to elucidate this relevant and practical problem.

REFERENCES

R.K. Bayer. The Force-Strain Relation of Extruded Polyethylene-Melts. *Rheol. Acta,* 18:25-32, 1979.

A. Bernnat. Polymer Melt Rheology and the Rheotens Test. Doctoral Thesis, 2001

M. M. Denn, *Computational Analysis of Polymer Processing*; Pearson, J. R. A., Richardson, S. M. Eds.; Applied Science Publishers: New York, 1983.

M.M. Denn. Issues in Viscoelastic Flow, *Ann. Rev. Fluid Mech*., 22:13-34, 1990.

R.Fulchiron, P Revenu., B.S. Kim, C. Carrot and J. Guillet. Extrudade Swell and Isothermal Melt Spinning Analysis of Linear Low Density Polyethylene Using the Wagner Constitutive Equation. *J. Non-Newtonian Fluid Mech*., 69:113-136, 1997.

H.H. George. Model of Steady-State Melt Spinning at Intermediate Take-Up Speeds, *Polym. Eng. Sci*., 22:292-299, 1982.

R.J. Gordon and W.R. Schowalter. Anisotropic Fluid Theory: a Different Approached to the Dumbbell Theory of Dilute Polymer Solutions, *Trans. Soc. Rheol.*, 16:79-97, 1972.

D.R. Gregory and M.T. Watson. Steady State Properties of Polyethylene Terephthalate Melts, *J. Polym. Sci*., 30:399-406, 1970.

G. M. Henson, D. Cao, S.E. Bechtel, and M.G. Forest. A Thin-Filament Melt Spinning Model with Radial Resolution of Temperature and Stress. *J. Rheol.* 42: 329-360, 1998.

H. M. Laun and H. Schuch. Transient Elongational Viscosities and Drawability of Polymer Melts. *J. Rheol*., 33:119-175, 1989.

G-G Lin and M-Ch Hu. Measurement of Elongation Viscosity for Polymer Melts by Fiber Spinning. *Advances in Polymer Technology,* 16:199-207, 1997.

C.W. Macosko. *Rheology: principles, measurements and applicatios*, VCH, 1994.

J. Meissner. Dehnungsverhalten von Polyethylen-Schmelzen. *Rheol. Acta*, 10:230-240, 1971.

M.L. Ottone and J.A. Deiber. Modeling the Melt Spinning of Polyethylene Terephthalate, *J. Elast. Plast.,* 32:119-139, 2000.

M.L Ottone and J.A. Deiber. A Numerical Method for the Viscoelastic Melt Spinning Model with Radial Resolutions of Temperature and Stress Field, *Industrial & Engineering Chemistry Research*, 41:6345-6353, 2002.

M.L. Ottone, M. B. Peirotti and J.A. Deiber. To be submitted, 2006.

T.C. Papanastasiou, V.D. Dimitriadis, L.E. Scriven, C.W. Macosko and R.L. Sani. On the Inlet Stress Condition and Admissibility Condition of Fiber Spinning. *Adv. Polym. Tech*., 15: 237-244, 1996.

C.J.S. Petrie. Extensional Flow-a Mathematical Perspective. *Rheol. Acta,* 34:12-26, 1995.

C.J.S. Petrie and A. Petrie. Spinning Viscosity. *J. Non-Newtonian Fluid Mech.,* 57:83-101, 1995.

V. Rauschenberger and H. M. Laun . A Recursive Model for Rheotens Tests. *J. Rheol*., 41:719-737, 1997.

P. Revenu, J. Guillet and Ch. Carrot. Elongational Flow of Polyethylenes in Isothermal melt Spinning. *J. Rheol*., 37:1041-1056, 1993.

T. Sridhar and R. K. Gupta. Material Properties of Viscoelastic Liquids in Uniaxial Extension. *J. Rheol*., 35:363-377, 1991.

M.H Wagner, B. Collignon and J. Verbeke. Rheotens Mastercurves and Elongational Viscosity of Polymer Melts. *Rheol. Acta*, 35:117-126, 1996.

M. H. Wagner, A. Bernnat and V. Shulze. The Rheology of Rheotens Test. *J. Rheol*., 42:917-928, 1998.